Role of Part-Inversion in Fluid-Structure Problems with Mixed Variables

BRUCE M. IRONS*
University of Wales, Swansea, Wales

REFERENCE 1 describes with examples a promising formulation for a linear elastic structure coupled to heavy compressible inviscid fluid;

$$\begin{bmatrix} -M & T \\ T^T & K_F \end{bmatrix} \begin{Bmatrix} \ddot{u} \\ p \end{Bmatrix} = \begin{bmatrix} K & O \\ O & M_F \end{bmatrix} \begin{Bmatrix} u \\ -\ddot{p} \end{Bmatrix} \quad (1)$$

Here $\ddot{u} = d^2u/dt^2$ is a vector of nodal accelerations, M and K are the mass and stiffness matrices for the structure, and u gives its nodal displacements. p gives the pressures at the nodes within the fluid and on the fluid-structure interface, and M_F and K_F are matrices such that the fluid behaviour alone can be represented by $M_F\ddot{p} + K_Fp = 0$. Thus M_F and K_F bear only a formal resemblance to M and K. T is a rectangular coupling matrix having a role as in Pian's early mixed-variable formulations.[2]

Equations (1) are also mixed in the unfortunate sense that time derivatives occur on both sides. This may be remedied by a partitioned solution which leads to natural frequency calculations[1] but this is somewhat cumbersome. However, the algebra by which the process was derived suggests a numerical technique which is elegant, instructive, and successful.

Our goal is to convert Eq. (1) to the normal form for a set of second-order, ordinary differential equations

$$[Q]\ \{\ddot{r}\} = \{r\}$$

Consider first the structural case $Mu = \lambda Ku$. Both M and K are represented in core as triangular matrices, being symmetric.[3] A solution procedure for solving this problem with an economical use of computer core storage has been suggested by Torson.[4] If K is positive-definite it can be over-written by its Cholesky square root L, a lower triangular matrix, where $K = LU$, $U = L^T$. The problem now reduces to one involving a single matrix, $Qv = \lambda v$ where $v = Uu$ and $Q = L^{-1}MU^{-1}$. The transformation to Q is achieved in two steps. First L is over-written by L^{-1}. Then M can be over-written by the triple product Q, starting at the final complete row and using an additional vector for temporary storage.[4] With Q and L^{-1} on core, v and λ are found by the Householder or power technique with little extra storage, and hence $u = U^{-1}v$.

The same approach extends to Eq. (1), which can be regarded symbolically as $M^*y = K^*z$. This transforms into $Q^*\{U^*y\} = \{U^*z\}$ which expands to

$$Q^* \begin{Bmatrix} U\ddot{u} \\ U_Fp \end{Bmatrix} = \begin{Bmatrix} Uu \\ -U_F\ddot{p} \end{Bmatrix} \quad (2)$$

where $M_F = L_FU_F$, $U_F = L_F{}^T$. Now Q^* may be further transformed by Asplund's part-inversion scheme[5]

$$\begin{bmatrix} Q_{11} & Q_{12} \\ Q_{21} & Q_{22} \end{bmatrix} \begin{Bmatrix} \ddot{v} \\ q \end{Bmatrix} = \begin{Bmatrix} v \\ -\ddot{q} \end{Bmatrix}$$

where $v = Uu$ and $q = U_Fp$

$$\therefore \begin{bmatrix} Q_{11} - Q_{12}Q_{22}^{-1}Q_{21}, & -Q_{12}Q_{22}^{-1} \\ -Q_{22}^{-1}Q_{21}, & -Q_{22}^{-1} \end{bmatrix} \begin{Bmatrix} \ddot{v} \\ \ddot{q} \end{Bmatrix} = \begin{Bmatrix} v \\ q \end{Bmatrix} \quad (3)$$

This is easily achieved in practice by interchanging one pair of variables, q_i and $\ddot{q}_i$, at a time, with no extra storage requirements. In essence this is the gaussian reduction process starting from the last row and working upwards, eliminating one variable at a time and rearranging the corresponding equation. Indeed, with N structural and n fluid degrees of freedom, the storage requirements can be reduced to $N^2 + Nn + n^2 + 2(N + n)$ words, apart from any special requirements of the eigenvalue routine. With the algorithms just described, the formulation therefore appears highly competitive.

Received July 28, 1969; revision received October 13, 1969.
* Lecturer, School of Engineering.

References

[1] Zienkiewicz, O. C. and Newton, R. E., "Coupled Vibrations of a Structure Submerged in a Compressible Fluid," *Proceedings of the International Symposium on Finite Element Techniques*, International Assoc. for Ship Structures, Stuttgart, June 1969.

[2] Pian, T. H. H., "Derivation of Element Stiffness Matrices by Assumed Stress Distributions," *AIAA Journal*, Vol. 2, No. 7, July 1964, p. 1333–1336.

[3] Anderson, R. G., Irons, B. M., and Zienkiewicz, O. C., "Vibrations and Stability of Plates Using Finite Elements," *International Journal of Solids and Structures*, Vol. 4, Oct. 1968, pp. 1031–1035.

[4] Torson, B. T., private communication, 1964, Rolls-Royce.

[5] Asplund, S. O., *Structural Mechanics: Classical and Matrix Methods*, Prentice-Hall, Englewood Cliffs, N.J., 1966.

Buckling of Truncated Conical Shells under Axial Compression

J. TANI* AND N. YAMAKI†
Tohoku University, Sendai, Japan

Introduction

THE elastic stability of truncated conical shells subjected to axial compression has been studied by several researchers.[1–4] In these studies, however, only approximate solutions are obtained by ignoring some of the boundary conditions. Recently, accurate solutions of this problem were obtained by Singer et al.[5] for simply supported shells, but clamped shells have not been treated.‡

In this paper, applying the same method as used for the corresponding problem under torsion,[6] the problem is accurately analysed under four sets of boundary conditions, including both clamped and simply supported cases. Through detailed calculations, the correlations to the buckling of equivalent cylindrical shells are clarified, which facilitates the estimation of critical load for any given conical shell. The results here obtained for simply supported cases are ascertained to be in good agreement with those obtained by Singer et al.[5]

Analysis

Assume that a truncated conical shell is subjected to the axial load P applied along the edges as shown in Fig. 1. Assuming the momentless state of stress for the prebuckling deformation, the Donnell type basic equations governing the critical state of the shell and the relations among the stress function, membrane forces, and displacements may be given in nondimensional form by[7]

$$\nabla^4 f + x^{-1}w_{,xx} = 0 \quad (1)$$

Received June 18, 1969; revision received November 4, 1969.
* Lecturer, Institute of High Speed Mechanics.
† Professor, Institute of High Speed Mechanics.
‡ After the completion of the present study, the authors were informed of the Singer paper through private communication.

Table 1 Relations between k_c and Z in each case: $\nu = 0.3$, $l/h = 100$

ρ_m/h		1.5×10^4	10^4	5×10^3	3×10^3	1.5×10^3	10^3	3×10^2
	Z	1.192	1.789	3.577	5.962	11.92	17.89	59.62
	C1	35.54(0)[a]	37.24(0)	46.28(0)	62.21(1)	104.0(2)	145.0(2)	430.0(4)
$\gamma = 0.2$	C2	34.67(0)	35.29(0)	38.66(0)	48.91(0)	82.98(1)	125.4(1)	413.6(3)
	S1	12.11(0)	14.36(0)	26.39(1)	45.24(1)	81.43(1)	124.7(2)	413.1(3)
	S2	14.21(1)	14.65(1)	16.98(1)	22.36(1)	44.01(1)	67.58(1)	213.6(1)
		12.00(0)[b]	14.11(0)					
	Z	3.816	5.724	11.45	19.08	38.16	57.24	190.8
	C1	120.8(0)	126.6(0)	156.0(1)	201.7(3)	330.6(4)	463.5(5)	1368(7)
$\gamma = 0.5$	C2	117.7(0)	119.6(0)	129.7(0)	153.8(0)	264.5(2)	399.1(4)	1323(7)
	S1	36.21(0)	44.01(0)	80.04(2)	134.8(3)	263.5(2)	397.6(5)	1321(8)
	S2	33.81(1)	35.20(1)	42.64(1)	59.76(1)	129.1(1)	205.9(1)	664.7(1)
	Z	28.62	42.93	85.85	143.1	286.2	429.3	1431
	C1	921.7(0)	965.5(0)	1183(5)	1521(8)	2457(12)	3595(9)	10240(10)
$\gamma = 0.8$	C2	897.5(0)	911.3(0)	986.2(0)	1165(1)	1983(6)	2976(10)	9910(7)
	S1	267.0(0)	329.6(0)	597.9(6)	999.3(9)	1984(6)	2977(11)	9919(8)
	S2	232.9(1)	243.3(1)	299.2(1)	428.0(1)	951.2(1)	1533(1)	4971(1)

[a] Numerals in parentheses indicate the number of circumferential waves.
[b] Numerals with underlines correspond to the combined boundary conditions of S1 and S2 as stated in the text.

$$L(w) \equiv \nabla^4 w - 12Z^2 x^{-1} f_{,xx} + k_c x^{-1} w_{,xx} = 0 \tag{2}$$

$$n_s = x^{-1} f_{,x} + x^{-2} f_{,\phi\phi},\ n_\theta = f_{,xx},\ n_{s\theta} = -(x^{-1} f_{,\phi})_{,x} \tag{3}$$

$$\left.\begin{aligned} u_{,x} = n_s - \nu n_\theta,\ x^{-1}(u + v_{,\phi} - w) = n_\theta - \nu n_s \\ x^{-1}(u_{,\phi} - v + x v_{,x}) = 2(1+\nu) n_{s\theta} \end{aligned}\right\} \tag{4}$$

where

$$\nabla^2 = \partial^2/\partial x^2 + (1/x)\partial/\partial x + (1/x^2)\partial^2/\partial\phi^2,\ \phi = \theta \sin\alpha \tag{5}$$

The notations in these equations are related to the usual ones as

$$\left.\begin{aligned} x = s/L,\ u = U/h \cot\alpha,\ v = V/h \cot\alpha,\ w = W/h \\ f = F/Eh^2 L \cot\alpha,\ (n_s, n_\theta, n_{s\theta}) = \\ (L/Eh^2 \cot\alpha)(N_s, N_\theta, N_{s\theta}) \\ Z = (1-\nu^2)^{1/2} L^2/\rho h,\ \gamma = L_0/L,\ k_c = PL^2/2\pi Dr \cos\alpha \end{aligned}\right\} \tag{6}$$

in which Z is a shape factor for the cone, γ is the truncation ratio and k_c is a load factor.

Concerning the boundary conditions, the following cases are considered where both edges are clamped, (C), and simply supported, for the deflection, (S) and where they are 1) constrained and 2) free for the in-plane displacements. Accordingly, at $x = \gamma$ and 1, the following conditions are obtained.

$$(C):\ w = w_{,x} = 0,\quad (S):\ w = w_{,xx} + \nu x^{-1} w_{,x} = 0 \tag{7}$$

$$1):\ u = v = 0,\ 2):\ n_s = n_{s\theta} = 0 \tag{8}$$

Combining these conditions, we will treat the four cases, which will be designated as cases C1, C2, S1, S2, respectively. The problem consists in finding the minimum characteristic value k_c of Eqs. (1) and (2), under the given boundary conditions.

To solve the problem we first assume w as

$$\left.\begin{aligned} w = \sum_m a_m w_m(x) \cos N\theta \\ w_m(x) = \sum_{j=0}^{4} c_{mj} x^{m+j}\ (m = 0,1,2,\ \ldots) \end{aligned}\right\} \tag{9}$$

where a_m are unknown parameters, N is the number of circumferential waves, and $c_{mj} (j = 0 - 4)$ are constants chosen so that w_m satisfies each supporting condition in Eq. (7) by taking c_{mo} as unity.

Substituting Eq. (9) into Eq. (1) and considering Eqs. (3) and (4), the stress function f can be determined so as to satisfy each stress condition in Eq. (8). With these expressions for w and f, we apply the Galerkin method to Eq. (2); that is,

$$\int_0^{2\pi} \int_\gamma^1 L(w) \sum_{k=0}^{4} c_{nk} x^{n+k+1} \cos N\theta d\theta dx = 0 \qquad n = 0,1,2,\ \ldots \tag{10}$$

which leads to the following system of homogeneous linear equations in a_m

$$\sum_m D_{nm} a_m = 0,\quad m,n = 0,1,2,\ \ldots \tag{11}$$

To have nontrivial solutions, the determinant of coefficients should vanish, i.e.,

$$\Delta \equiv |D_{nm}| = 0 \tag{12}$$

When the values for ν, γ, l/h, and $\rho_m/h = (\rho + \rho_0)/2h$ are given, Δ depends on only N and k_c. Hence, we can determine from Eq. (12) the minimum value of k_c and the corresponding value of N, which represent the critical load and the number of buckled waves, respectively.

Now, we will consider the special case for the axisymmetrical buckling. The basic equations for this case are given by

$$x u_{,xx} + u_{,x} - x^{-1} u = \nu w_{,x} - x^{-1} w \tag{13}$$

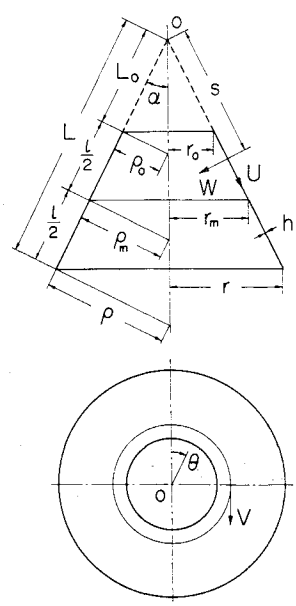

Fig. 1 Coordinates and nomenclature of the truncated conical shell.

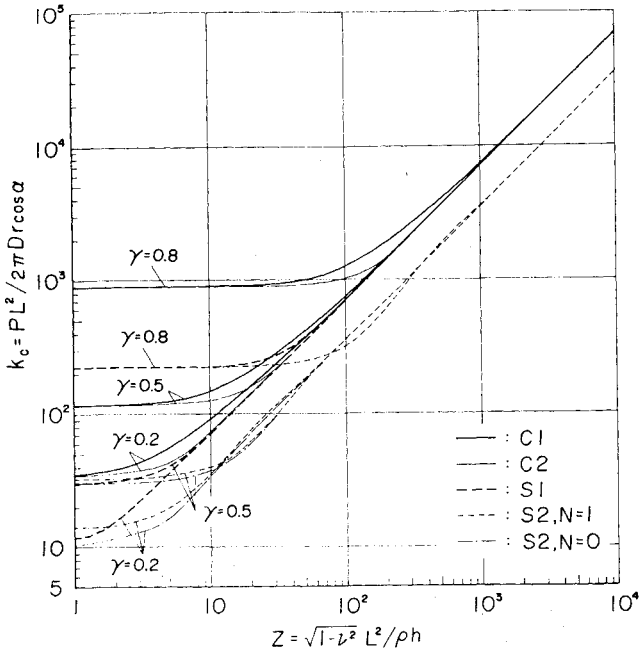

Fig. 2 Relations between k_c and Z in each case.

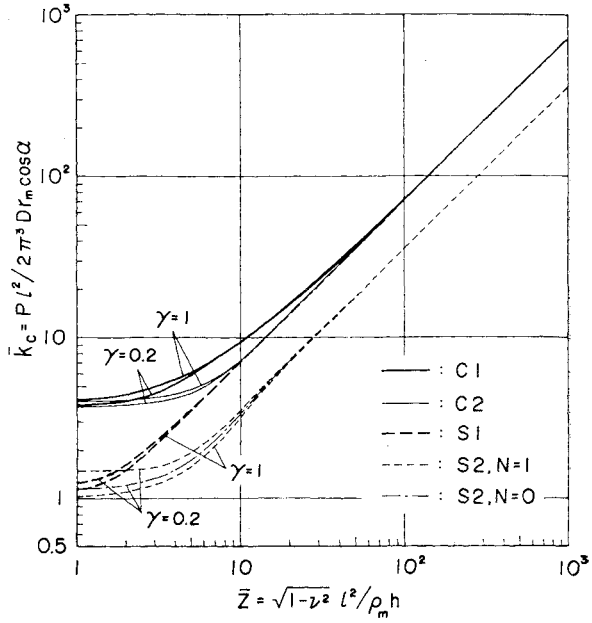

Fig. 3 Relations between $\bar{k}_c$ and $\bar{Z}$ in each case.

$$w_{,xxxx} + 2x^{-1}w_{,xxx} - x^{-2}w_{,xx} + x^{-3}w_{,x} - [12/(1-\nu^2)]Z^2x^{-2}(u - w + \nu x u_{,x}) + k_c x^{-1}w_{,xx} = 0 \quad (14)$$

For the boundary conditions, the supporting conditions are given by Eq. (7) as before, while the stress conditions become

$$1)\ \ u = 0, \quad 2)\ u_{,x} + \nu x^{-1}u = 0 \quad (15)$$

The deflection w is expressed by Eq. (9) with $N = 0$. Substituting this into Eq. (13), u is determined so as to satisfy each stress condition in Eqs. (15). Applying the Galerkin method to Eq. (14), the critical load can be determined in the same way as mentioned in the foregoing.

Numerical Results

Assuming $\nu = 0.3$, $l/h = 100$, $\gamma = 0.2, 0.5, 0.8$, and varying the values for ρ_m/h from 10 to 5×10^4, critical values of k_c and N in each case are determined for the various values of Z ranging from 1 to 10^4. The convergency seems to become worse with the decrease in γ and increase in Z. In the worst case, it requires 13 terms of a_m to obtain fairly accurate results with error less than 1%. The main results are given in Table 1, which are shown in Fig. 2. In this figure, variations of k_c with γ are so great that it is difficult to estimate the critical value for any given value of γ. Therefore, the following parameters are introduced:

$$\bar{Z} = \frac{2(1-\gamma)^2}{1+\gamma} Z = (1-\nu^2)^{1/2}\frac{l^2}{\rho_m h}, \qquad \bar{k}_c = \frac{2(1-\gamma)^2}{\pi^2(1+\gamma)} k_c = \frac{Pl^2}{2\pi^3 Dr_m\cos\alpha} \quad (16)$$

where $r_m = (r + r_o)/2$. For circular cylindrical shells, these notations reduce to the well-known ones proposed by Batdorf.[8]

The relations between $\bar{k}_c$ and $\bar{Z}$ in each case are shown in Fig. 3. In this figure, curves labelled with $\gamma = 1$ correspond to accurate solutions for circular cylindrical shells obtained by Yamaki et al.[9] Curves for $\gamma = 0.5$ and 0.8 are omitted as they are so close to those for $\gamma = 1$. It will be seen that edge clamping effect is significant for short shells with $\bar{Z}$ less than 10. Further, it is found that in the cases C1, C2, and S1, the axisymmetrical buckling appears for $\bar{Z}$ less than 3, 10, and 2, respectively, and that for $\bar{Z}$ larger than 30, the buckling loads are almost coincident with the so-called classical values, i.e., $P_{cr} = 2\pi Eh^2\cos^2\alpha/[3(1-\nu^2)]^{1/2}$.

In the case S2, it is found that theoretically the axisymmetric buckling mode with $N = 0$ corresponds to the lowest critical load in the range here calculated. The results are shown in Figs. 2 and 3 by chain lines. However, this case is excluded, because it leads to a large axial translation of the shell as pointed out by Singer.[10] Then, the asymmetric buckling mode with $N = 1$ corresponds to the critical buckling load, as in the buckling of circular cylindrical shells in the case S2.[9] The corresponding results are shown by fine dotted lines. It is found that for large values of γ or Z, the results for $N = 1$ are almost coincident with those for $N = 0$, which are nearly half the classical buckling loads. In the other case, for example, $\gamma = 0.2$, $Z < 2$, and $\gamma = 0.5$, $Z < 3$, these become higher than the axisymmetric buckling loads for the case S1. Hence, for reference, the axisymmetric buckling is considered under the new boundary condition combining S1 and S2, i.e., $u = 0$ at $x = 1$ and $u_{,x} + \nu x^{-1}u = 0$ at $x = \gamma$. The results thus obtained are not shown in the figures as they are only slightly smaller than those for case S1.

References

[1] Seide, P., "Axisymmetrical Buckling of Circular Cones Under Axial Compression," *Journal of Applied Mechanics*, Vol. 23, No. 4, 1956, pp. 625–628.

[2] Lackman, L. and Penzien, J., "Buckling of Circular Cones Under Axial Compression," *Journal of Applied Mechanics*, Vol. 27, No. 3, 1960, pp. 458–460.

[3] Seide, P., "On the Stability of Internally Pressurized Conical Shells Under Axial Compression," *Proceedings of the 4th U.S. National Congress of Applied Mechanics*, Univ. of Calif., Berkeley, June 1962, pp. 761–773.

[4] Singer, J., "Buckling of Circular Conical Shells under Uniform Axial Compression," *AIAA Journal*, Vol. 3, No. 5, May 1965, pp. 985–987.

[5] Baruch, M., Harari, O., and Singer, J., "Low Buckling Loads of Axially Compressed Conical Shells," TAE Rept. 76, Jan. 1968, Technion Research and Development Foundation, Haifa, Israel.

[6] Yamaki, N. and Tani, J., "Buckling of Truncated Conical Shells under Torsion," *Zeitschrift für Angewandte Mathematik und Mechanik*, Vol. 49, No. 8, 1969, pp. 471–480.

[7] Seide, P., "A Donnell Type Theory for Asymmetrical Bending and Buckling of Thin Conical Shells," *Journal of Applied Mechanics*, Vol. 24, No. 4, 1957, pp. 547–552.

[8] Batdorf, S. B., "A Simplified Method of Elastic Stability Analysis for Thin Cylindrical Shells," Rept. 874, 1947, NACA, pp. 285–309.

[9] Yamaki, N. and Kodama, S., "Buckling of Circular Cylindrical Shells under Axial Compression," to be published in the Reports of the Institute of High Speed Mechanics, Tohoku Univ., Japan.

[10] Baruch, M., Harari, O., and Singer, J., "Addendum to TAE Report 76, Low Buckling Loads of Axially Compressed Conical Shells," March 1969, Technion Research and Development Foundation, Haifa, Israel.

Tapered Resonance Tubes: Some Experiments

ROBERT F. MCALEVY III*

AND

ALEX PAVLAK†

Stevens Institute of Technology, Hoboken, N. J.

Introduction

IN 1916 Hartmann[1] discovered that under appropriate conditions intense noise emanated from, and pressure oscillations were produced in, shallow circular-cylindrical cavities of uniform cross-sectional area placed in sonic airjets. Now known as the Hartmann whistle, this device has been subjected to extensive investigation directed towards improvement of its acoustic efficiency[2] (Fig. 1a).

In 1954 Sprenger[3] discovered that under appropriate conditions a very slender Hartmenn whistle, with a length-to-diameter ratio, l/d, of 34 in contrast to a nominal l/d of about 4, exhibited intense heating at the closed end. Now known as the resonance tube, (Figure 1b), this device is a less efficient noise generator than the Hartmann whistle, but is of interest due to its heating characteristics. Sprenger recorded average resonance tube end-wall temperatures as high as 840°F with clean air and 1830°F when solder particles were accidentally introduced into the driving airstream. The generation of temperatures several times greater than the free-stream stagnation temperature by a simple passive device appears to be unique.

It is believed that the underlying aerodynamic resonance phenomenon might contribute, under certain conditions, to enhanced meteorite "pitting" and ablation of heat shields on atmospheric re-entry vehicles, as well as thermally induced structural failure in a number of devices of technological interest, e.g., pneumatic systems. Further, it represents a potential explosion hazard, as has been recognized in the past.[4] Simple laboratory experiments illustrate graphically this aspect. For example, a small slug of wood placed in a resonance tube will ignite and burn vigorously in a few seconds.[3,4] Indeed, there has been an attempt to harness this explosive potential in a passive ignition system for hydrogen-oxygen rocket engines.[5]

All previous investigations of the phenomenon known to the authors were restricted to resonance tubes of uniform cross section along the entire length. By contrast, the subject study dealt primarily with tubes that were unique by virtue of having cross-sectional area distributions which decreased continuously from the open mouth to zero area at the closed end, i.e., tapered tubes (Fig. 1c). In practical situations that hold explosion hazards, such as incipient failure of pneumatic system seals, it is believed that tapered resonance tubes approximate the actual geometries better than do the conventional tubes previously studied.

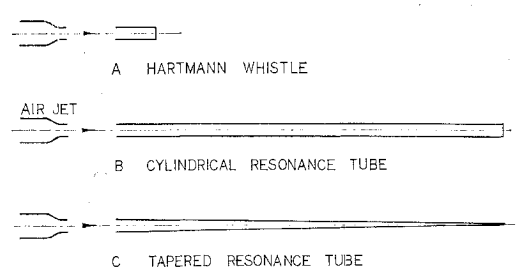

Fig. 1 Schematic of Hartmann whistle and resonance tubes.

Aerodynamic Phenomena of the Uniform Cross Section Resonance Tube

Instability has been found to be excited by sonic and supersonic airjets[6] and by subsonic and supersonic wind-tunnel flows. The most widely used method of excitation for experimental investigation has been sonic airjets.

The first realistic description of the fully developed flow within conventional resonance tubes was produced by Thompson.[6] By using a correctly expanded supersonic airjet he produced experimentally well-defined boundary conditions at the mouth, which enabled him to construct a wave diagram for the internal flowfield. This was well supported by experimentally observed pressure histories and flow patterns within the tube.

Thompson and others observed that the conventional tubes resonated at approximately the acoustic (simple organ pipe) frequency based on the freestream stagnation temperature. During part of the cycle some of the airjet gas is ingested, and much of the same gas is expelled during the remainder of the cycle. Thus, a slug of indigenous gas is trapped near the endwall for many cycles.

On every cycle a system of shock waves and expansion waves of nonuniform strength transit the indigenous slug. As the local entropy increase during compression is greater than the local decrease during expansion, it follows that the net thermal effect of a cycle is to produce an incremental increase of local temperature. Since resonance tubes operate at several hundred cps, even a small temperature increment per cycle can result in rapid heat-up of the indigenous gas; in extreme cases reaching temperatures far in excess of 1000°F within several seconds. No valid means of predicting resonance tube thermal effects are known to the authors. For example, not even the maximum temperature theoretically possible in the adiabatic situation, i.e., no heat loss to the surroundings from the tube, can be realistically predicted.[8]

Description of the Experiment

A variety of combinations of airjet velocity, ratio of airjet nozzle diameter to resonance tube diameter, resonance tube l/d, and separation between airjet nozzle and tube mouth have been found to produce the aerodynamic resonance of interest.[3] As the thermal effects were of prime interest in the present study, a configuration was selected that maximized it. That is, an airjet, produced by expanding from stagnation conditions of 70 psig and 70°F through a converging nozzle of $\frac{5}{16}$ in. diam to the atmosphere, was used for driving axially aligned tubes of $\frac{5}{16}$ in. diam area located $1\frac{1}{4}$ in. away. The tubes were all about $10\frac{1}{4}$ in. long. (Experimental details are

Received September 8, 1969; revision received October 27, 1969. Mechanical Engineering Department funds partially supported this work. The authors would like to acknowledge the help of A. Cerkanowicz who developed much of the resonance tube testing facility and discussed with them on several occasions the subject work.

* Director, Combustion Laboratory. Member AIAA.

† Graduate Student; now at MSD, General Electric, King of Prussia, Pa.